Chapter one: Introduction

1.1. Introduction:

X-rays are electromagnetic waves or photons not emitted from the nucleus, but normally emitted by energy changes in electrons x-rays are radiations possessing high energy and penetrating capacity. They are classified as ionizing radiation and are extensively used for industrial, medical diagnostic and therapeutic purposes. Digital radiography is becoming a standard technique, due to better quality of images and reduced patient dose. In order to avoid unnecessary radiation dose to the patient, recent experience has shown that there is a need to consider many factors, some of which were not considered in analogue techniques. It is important to keep the radiation doses to patients at a minimum, because the use of X-rays in medicine for diagnosis represents the largest man-made source of public exposure to ionizing radiation. (Murat Beyzadeoglu et al , 2010).

In X-ray tubes, the heel effect or anode heel effect is a variation of the intensity of X-rays emitted by the anode depending on the direction of emission. Due to the geometry of the anode, X-rays emitted towards the cathode are in general more intense than those emitted perpendicular to the cathode–anode axis. The effects stems from the absorption of X-ray photons before they leave the anode in which they are produced. The probability for absorption depends on the distance the photons travel within the anode material, which in turn depends on the direction of emission.

An X-ray flux irradiation intensity distribution which is non uniform due to a heel effect can be made uniform, and a subject can be prevented from being Unnecessarily exposed. In addition, image quality of image data obtained

with an conventional X-ray can be made uniform and improved in a body axis direction. (Curry TS, et al, 1990)

1.2. Problem of the study:

The heel effect causes an angular dependence of the emitted spectrum and has been known in x-ray radiology for a long time. Artifacts due to the heel effect have been observed in radiography but only resulted in a slightly varying dose distribution in conventional x-ray radiology.

1.3. Objectives:

1.3.1. General objective

Evaluation of conventional x-ray machine heel effect.

1.3.2. Specific objectives:

-To estimate reduction of x-ray intensity to cathode and anode.

-To evaluate the heel effects of radiography.

-To check application of anode heel effects of radiographer.

1.4. Over view of the thesis:

This study falls into five chapters, Chapter one, which is an introduction, deals with theoretical frame work of the study, It presents the statement of the study problems, objectives of the study, chapter two deals with radiological physics and back ground. Chapter three deal with material and method, Chapter four deals with results and discussions. Chapter five conclusion , recommendations and references.

Chapter two
Literature Review

2.1 Radiation:

The propagation of energy from a radiative source to another medium is termed radiation. This transmission of energy can take the form of particulate radiation or electromagnetic radiation (i.e., electromagnetic waves). The various forms of radiation originating from atoms, which include (among others) visible light, X-rays and γ-rays, are grouped together under the terms “electromagnetic radiation" or “the electromagnetic spectrum". Radio waves, which have the longest wavelengths and thus the lowest frequencies and energies of the various types of electromagnetic radiation, are located at tone end of the electromagnetic spectrum, whereas X-rays and γ-rays, which have the highest frequencies and energies, are situated at the other end of this spectrum. (Pam Cherry et al,2009).

2.2 Classification of Radiation:

Radiation is classified into two main categories: *non ionizing* and *ionizing*, depending on its ability to ionize matter. The ionization Potential of atoms, *i.e*., the minimum energy required for ionizing an atom, ranges from a few eV for alkali elements to 24.6 eV for helium (noble gas).

• *Non*-ionizing radiation cannot ionize matter because its energy is lower than the ionization potential of matter.

• Ionizing radiation can ionize matter either directly or indirectly because its energy exceeds the ionization potential of matter. It contains two major categories:

– Directly ionizing radiation (charged particles) electrons, protons, alpha particles, heavy ions

– Indirectly ionizing radiation (neutral particles) photons (x rays, gamma rays), neutrons

Directly ionizing radiation deposits energy in the medium through direct Coulomb interactions between the directly ionizing charged particle and orbital electrons of atoms in the medium.

Indirectly ionizing radiation (photons or neutrons) deposits energy in the medium through a two step process:

- In the first step a charged particle is released in the medium (photons release electrons or positrons, neutrons release protons or heavier ions).
- In the second step, the released charged particles deposit energy to the medium through direct Coulomb interactions with orbital electrons of the atoms in the medium.

Both directly and indirectly ionizing radiations are used in treatment of disease, mainly but not exclusively malignant disease. The branch of medicine that uses radiation in treatment of disease is called *radiotherapy*, *therapeutic radiology* or *radiation oncology*. *Diagnostic radiology* and *nuclear medicine* are branches of medicine that use ionizing radiation in diagnosis of disease. (Pam Cherry et al, 2009).

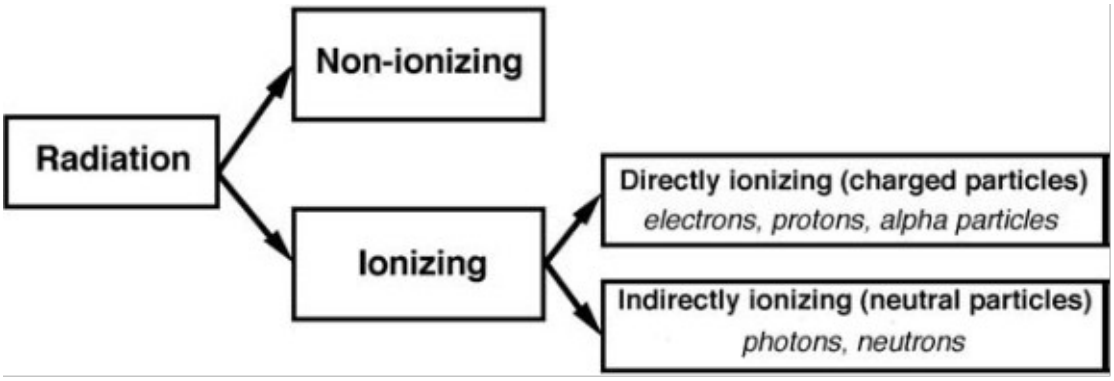

The figure2.1 shows the types of radiation. (E.B. Podgorsak, 2005)

2.3 Types and Sources of Directly Ionizing Radiation:

Directly ionizing radiation consists of several groups of charged particles, such as light charged particles (electrons and positrons), heavy charged particles (protons, deuterons, and alpha particles), and heavier charged particles (e.g.,carbon-12).

2.3.1 Electrons:

Electrons play an important role in medical physics. They are used directly as beams for cancer therapy, they are responsible for the dose deposition in media by photon and electron beams, and they govern the experimental and theoretical aspects of radiation dosimetry.

- Electrons released in medium by photoelectric effect are referred to as

photoelectrons.

- Electrons released in medium by Compton effect are referred to as *Compton* or

recoil electrons.

- Electrons produced in medium by pair production interactions in the field of the nucleus or in the field of an orbital electron are referred to as *pair production electrons.*

- Electrons emitted from nuclei by $\beta-$ radioactive decay are referred to as

beta particles.

• Electrons produced by linear accelerators (linacs), betatrons or microtrons for use in radiotherapy with kinetic energies typically in the range from 4 MeV to 30 MeV are referred to as *megavoltage electrons.*

- Electrons produced through Auger effect are referred to as *Auger electrons*,

Coster-Kronig electrons or *super Coster-Kronig electrons*.

- Electrons produced through internal conversion are referred to as *internal conversion electron*

- Electrons produced by charged particle collisions are of interest in radiation dosimetry and are referred to as *delta (δ) rays*. (E.B. Podgorsak, 2005).

2.3.2 Positrons:

Positrons produced by pair production or triplet production are referred to as pair production positrons, Positrons emitted from nuclei by β+ radioactive decay are used in positron emission tomography (PET) and referred to as beta particles. (E.B. Podgorsak, 2005)

2.3.3 Heavy Charged Particles:

Heavy charged particles are produced for use in radiotherapy through acceleration of nuclei or ions in cyclotrons, synchrotrons or heavy particle linacs: *Proton*: nucleus of hydrogen-1 ($_1$H) atom, *Deuteron*: Nucleus of deuterium (21 H) atom that consists of a proton and a neutron bound together with a total binding energy of 2.22 Mev, *Triton*: Nucleus of tritium (31H) atom consisting of one proton and two neutrons bound together with a total binding energy of 8.48 Mev.

Helium-3: Nucleus of helium-3 (32He) atom consisting of 2 protons and 1 neutron bound together with a total binding energy of 7.72 Mev.

α particle: Nucleus of helium-4 (42He) atom consisting of 2 protons and 2 neutrons bound together with a total binding energy of 28.3 Mev.

2.4 Classification of Indirectly Ionizing Photon Radiation:

Indirectly ionizing photon radiation consists of four distinct groups of photons: *Characteristic (fluorescent) x rays* result from electron transitions between atomic shells, *Bremsstrahlung photons* result from electron-nucleus Coulomb interactions, *Gamma rays* result from nuclear transitions, *Annihilation quanta* result from positron-electron annihilation. (E.B. Podgorsak, 2005).

2.5. X-ray Production:

2.5.1. The X-ray tube:

Within an X -ray tube, X -rays are produced when electrons with kinetic energy impact upon a high -density target. Each component part of the X -ray tube has been designed with the desire to produce electrons, supply them with energy and enable an efficient as possible interaction with a target. The aim is to provide a small area on the target, where X -rays are emitted (the focal spot), with a high - intensity beam. This has to be traded off with the large amount of heat produced in the anode as a byproduct. This section looks at the function of each component of an X - ray tube. Figure 2.1 shows a diagram of the components of an X -ray tube. This tube consists of a cathode and an anode enclosed within an evacuated glass or metal envelope. This is all contained within lead - shielded housing, which also contains oil to remove heat from the X -ray tube. high voltage is applied across the tube by a generator (Pam Cherry et al, 2009).

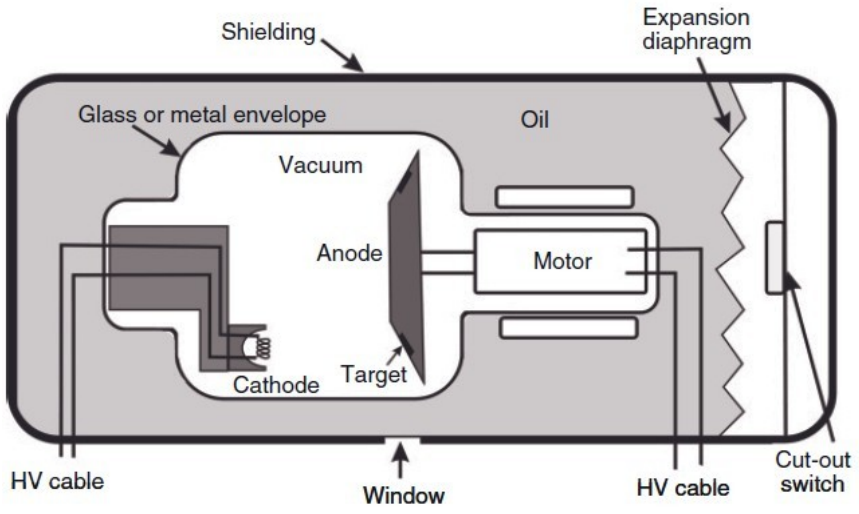

Figure 2.2 A diagram of an X -ray tube (Pam Cherry et al, 2009).

2.5.1.1 Cathode:

The cathode is the negatively charged electrode, where electrons are released into the X -ray tube. This is the start of the X -ray production process and consists of two parts: a filament and a focusing cup. The filament is a coil of tungsten wire, which is about 2 mm in diameter.

It is tightly coiled, similar to the heating element in a bar heater or a toaster, in order to increase the surface area of the metal. A very high current is passed through this coil, which heats the metal to such an extent that the outer electrons of the tungsten atoms are boiled off, and ejected from the surface of the coil. This phenomenon is known as thermionic Tungsten is a good material for this purpose because it has a high melting point and high thermal conductivity. This means that it can heat and cool quickly, allowing it to be heated rapidly for thermionic emission, and it can with stand high temperatures without becoming damaged. The rate at which the electrons are emitted by the cathode is directly

related to the tube current. When electrons are produced by the cathode coil they spread out, because their negative charges electrostatically repel each other. This would result in some electrons not reaching the target, which would reduce the efficiency of the tube. To stop this from happening a focusing cup is used, which is a negatively charged block of nickel that shapes the electrons coming from the filament into a focused beam, and hence a small area on the target (Pam Cherry et al, 2009).

2.5.1.2 High voltage:

The tube current flows from the cathode to the positively charged anode. A high voltage is supplied across the tube in order to accelerate the electrons and increase their kinetic energy. This voltage is the kilovolt (kV) setting of the tube and is supplied by a generator, which is separate from the X -ray tube (Pam Cherry et al, 2009).

2.5.1.3 Anode:

The anode is the positively charged electrode, directly opposing the cathode. It consists of ahigh - density metal target, embedded in a copper disc. The electrons

from the cathode hit the target area of the anode and interact. Tungsten is usually chosen as a target material. This is due to the useful properties of this material. First, it has a high density, which increases the number of interactions per projectile electron. It also has a high melting point, allowing the target to become very hot without becoming damaged, and last it has a high thermal conductivity. This means the heat generated in the target is quickly dissipated to the surrounding copper, which acts as a heat sink for the anode. Most tubes have a rotating anode. This is to increase the efficiency of removing heat from the target area during the

production of X - rays, which makes it possible to produce a higher - intensity beam without damaging the area of the anode struck by the projectile electrons. Some industrial, dental and small mobile units have stationary anodes. A stationary anode tube is Cheaper to manufacture and easier to maintain; however, it cannot be used when a high power output is needed (Pam Cherry et al, 2009).

2.5.1.4 Focal spot size:

The area where the electron current hits the target is known as the focal spot. The smaller the focal spot, the greater the resolution of the image produced with the tube. However, with a small focal spot the amount of heat transferred to the target by the electrons becomes concentrated in a small area. If the heat from the target cannot be dissipated fast enough the target may become damaged and crack, causing the tube to fail. Apart from using a rotating anode a good way to reduce the focal spot size is to utilize the angle of the anode. The actual focal spot size is the area of the target that interacts with the electron beam. The angle of the anode means that the X -ray beam exiting the tube is much smaller than this area. This is called the line focus principle and is illustrated in Figure 2.2. The angle marked is known as the target angle. (E.B. Podgorsak, 2006)

2.5.1.5 Envelope:

The cathode and anode are housed inside a glass or metal envelope. The envelope is sealed, and maintained at vacuum pressure. This is necessary so that the electrons can travel from the cathode to the anode without losing any energy during unwanted interactions with air molecules. The envelope was traditionally made of glass, because this is an easy material to mould and it is resistant to high temperatures. More modern tubes have housing made from metal. This does not degrade over time in the same way that glass does and so increases the lifetime of the tube (Pam Cherry et al, 2009).

2.5.1.6 Housing:

The envelope is in turn contained inside sturdy housing, which has several purposes. It provides protection and support for the components of the X -ray tube. There is a low attenuation window where the radiation beam exits towards the patient. The housing is filled with oil, which is used to dissipate heat from the anode. The oil expands as it heats up, and if this expansion becomes too great a cut

-off switch is activated to prevent the tube from overheating. The housing is also coated in lead to provide shielding, and prevent radiation from being given off in any direction except the window. Finally filters and collimators can be attached to this housing (Pam Cherry et al, 2009).

2.5.1.6 Motor:

The motor rotates the anode using electromagnetic induction. This type of motor allows the anode to be powered, while the envelope containing the anode can still be sealed.

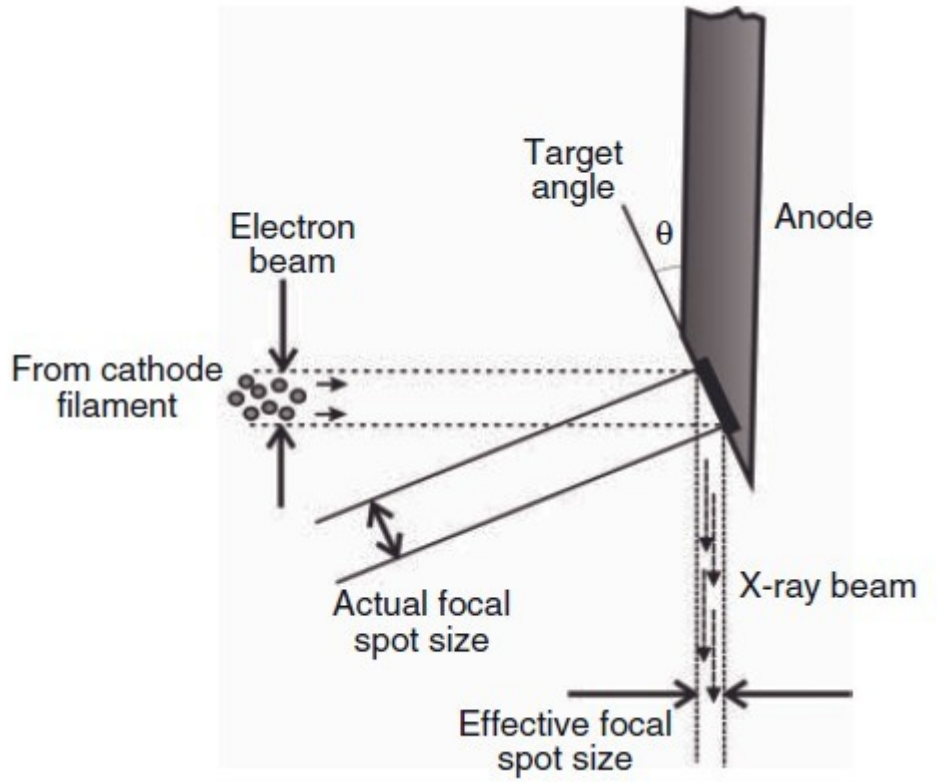

Figure 2.3 The effective focal spot size of an X – ray tube. (Pam Cherry et al, 2009).

2.5.2 X-Rays:

X-rays were discovered by the German physicist Wilhelm Conrad Roentgen in The hot cathode Roentgen tube, which was developed by William David Coolidge in

1913, is a pressured (to 10−3 mmHg) glass tube consisting of anode and cathode layers between which a high-energy (106 –108 V) potential is applied . Electrons produced by thermionic emission in the cathode are accelerated towards the anode by the potential. They thus hit the anode, which is a metal with high melting temperature. X-rays are produced by the sudden deceleration of these electrons due to Coulomb interactions with nuclei in the anode (this sudden deceleration of fast-moving electrons is known as bremsstrahlung). The energy and the wave

Length of the X rays depend on the atomic number of the target (anode) metal, as well as the velocity and the kinetic energy of the electrons. This process is used to produce medical radiation in diagnostic X-ray units, linear accelerators (linacs), and betatrons.

X-rays are produced by extra nuclear procedures. Two kinds of X-rays are created by X-ray tubes . The first type corresponds to the bremsstrahlung X-rays mentioned above. The second type occurs because an electron in an inner atomic orbital is knocked out by an incoming electron, and the resulting space in the orbital is filled by other electron that moves from an outer atomic orbital . This electron must shed energy to move in this manner, and the energy released is radiated as characteristic X-rays . They are characteristic due to the fact that their energy depends on the target metal onto which the electrons are accelerated.

X-rays produced by bremsstrahlung have a broad energy spectrum (heterogeneous), while characteristic X-rays are monoenergetic beams (Murat Beyzadeoglu et al , 2010).

2.6 interaction of radiation with matter:

2.6.1 Rayleigh Scattering:

In Rayleigh scattering, the incident photon interact with and excites the total atom , as opposed to individual electrons as in Compton scattering or the photoelectric effect , this interaction occurs mainly with very low energy diagnostic x-rays as used in mammography.

During the Rayleigh scattering event, the electric field of the incident photons electromagnetic wave expends energy causing all of the electrons in the scattering atom to oscillate in phase.

The atoms electron cloud immediately radiates this energy, emitting a photon of the same energy but in a slightly different direction .In this interaction, electrons are not ejected and thus ionization does not occur. In general the scattering angle increases as the x-ray energy decrease. (Murat Beyzadeoglu et al , 2010).

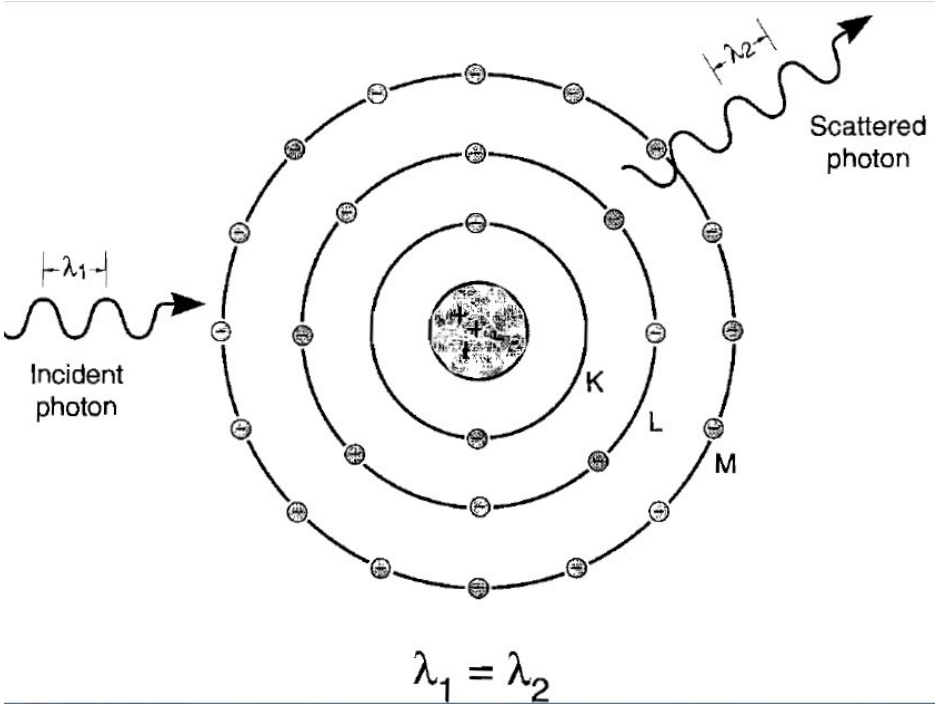

the figure2.4 show the Rayleigh scattering (Bushberg JT et al , 2002).

2.6.2. Photoelectric Effect

This phenomenon, which was theorized by Albert Einstein in 1905, was actually first observed by Heinrich Rudolf Hertz in 1887, and was therefore also known as the Hertz effect. To define it simply, when any electromagnetic radiation reaches a surface (generally a metallic surface), it transfers its energy to the electrons of that surface, which are then scattered. At the atomic level, the incoming radiation knocks an electron from an inner atomic orbital, propelling it from the atom (Fig.

2.5).

This is the basic interaction in diagnostic radiology.

It is dominant at energies of less than 35 kV, and in atoms with high atomic numbers (*Z*). Since the atomic number of bone is higher than that of soft tissue,

bone absorbs more radiation than soft tissue. This absorption difference is the basis of diagnostic radiology.

This effect also explains why metals with high atomic numbers (e.g., lead) are used to absorb low-energy X-rays and gamma rays.

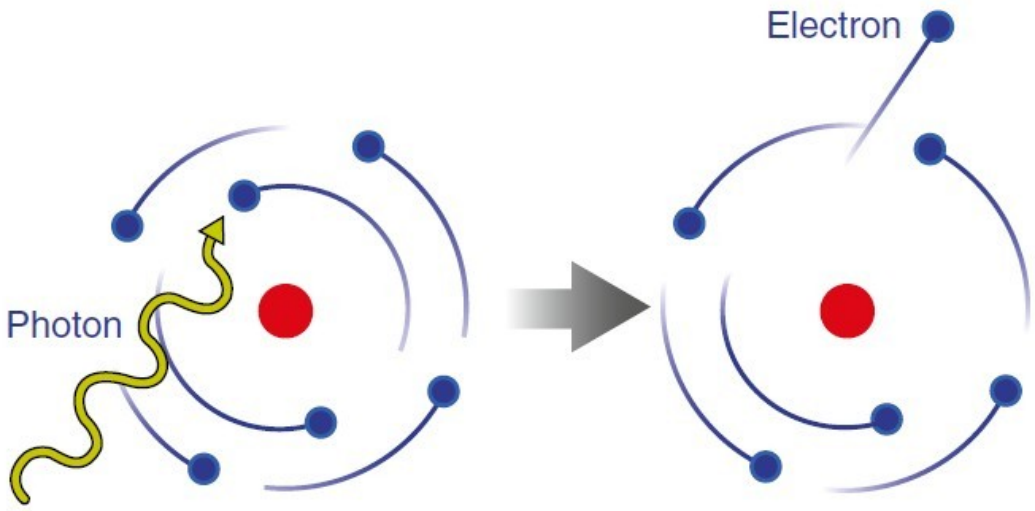

The figure2.5 show the illustration of photoelectric effect. (Murat Beyzadeoglu et al , 2010).

2.6.3 Compton Effect:

In the Compton effect, a photon collides with an electron in an outer orbital, and the photon and electron are scattered in different directions (where q is the angle between the directions).

The energy of the incoming photon is transferred to the electron in the form of kinetic energy. The scattered electron also interacts with the outer orbital electrons of other atoms. After the interaction, the photon has a lower energy than it did beforehand. (Murat Beyzadeoglu et al, 2010).

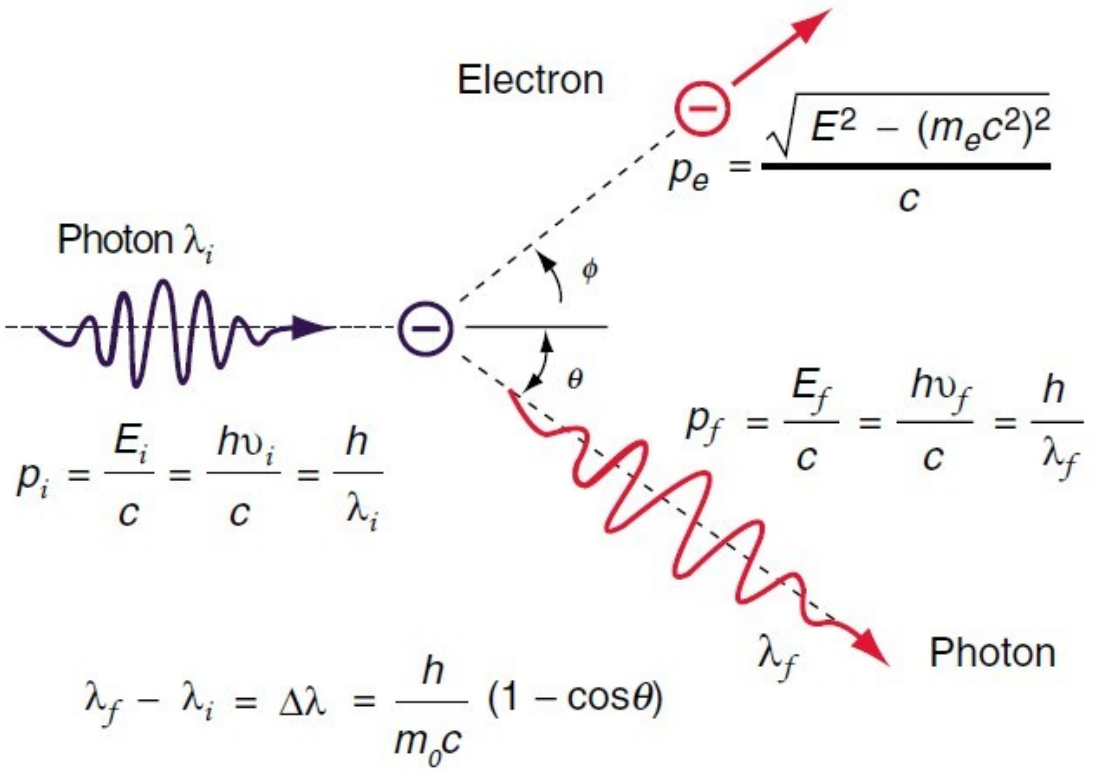

Fig. 2.6 Math associated with the Compton Effect. (Murat Beyzadeoglu et al , 2010).

This is the main mechanism for the absorption of ionizing radiation in radiotherapy. It is the dominant effect across a wide spectrum of energies, such as 35 kV–50 MV.

It has no dependency on the atomic number (*Z*) of the absorbent material, but it does depend on the electron density of the material.

The absorption of incoming radiation is the same for bone and soft tissues.

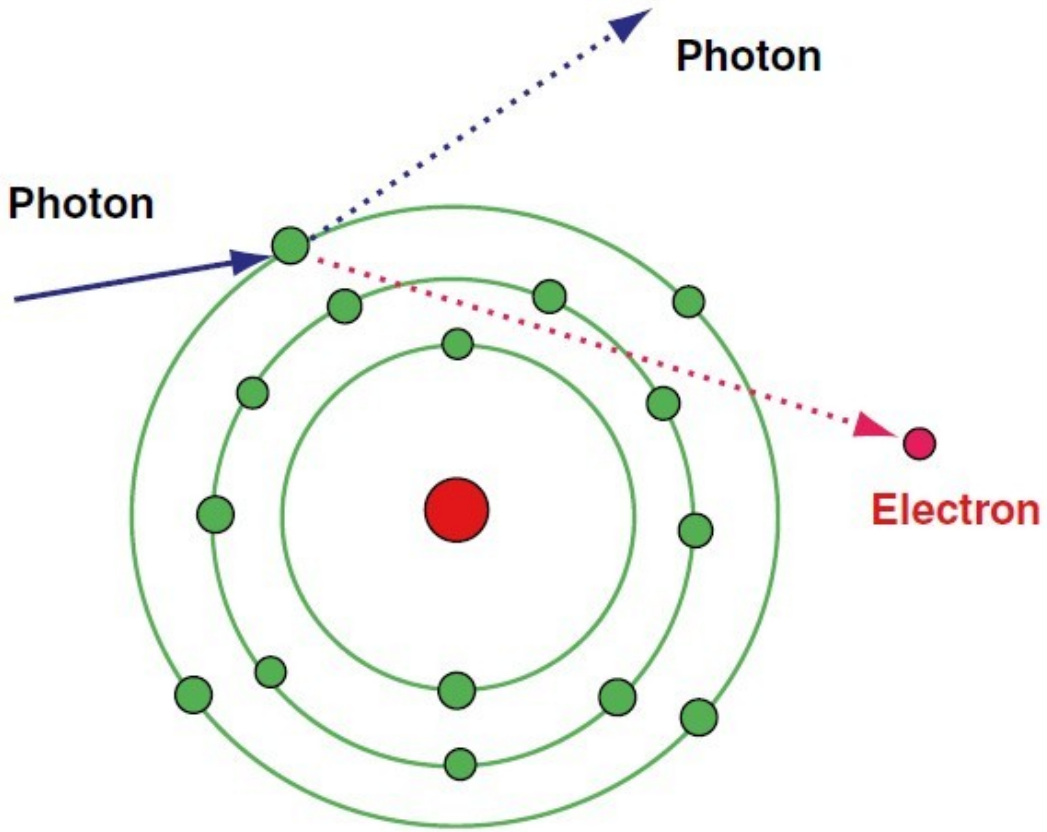

Fig. 2.7 Illustration of the Compton Effect. (Murat Beyzadeoglu et al , 2010).

2.6.4 Pair Production:

Pair production can only occur when the energies of x-rays and gamma rays exceed 1.02 MeV. In pair production, an x-or gamma ray interacts with the electric field of the nucleus of an atom. The photon's energy is transformed into an electron-positron pair (Fig. 2.8). The rest mass energy equivalent of each electron is 0.511 MeV and this is why the energy threshold for this reaction is 1.02 MeV. Photon energy in excess of this threshold is imparted to the electrons as kinetic energy.

The electron and positron lose their kinetic energy via excitation and ionization. As discussed previously, when the positron comes to rest, it interacts with a negatively

charged electron, resulting in the formation of two oppositely directed 0.511 MeV annihilation photons (Fig. 2.8).

Pair production is of no consequence in diagnostic x-ray imaging because of the extremely high energies required for it to occur. In fact, pair production does not become significant unless the photon energies greatly exceed the 1.02 MeV energy thresholds. (E.B. Podgorsak, 2006)

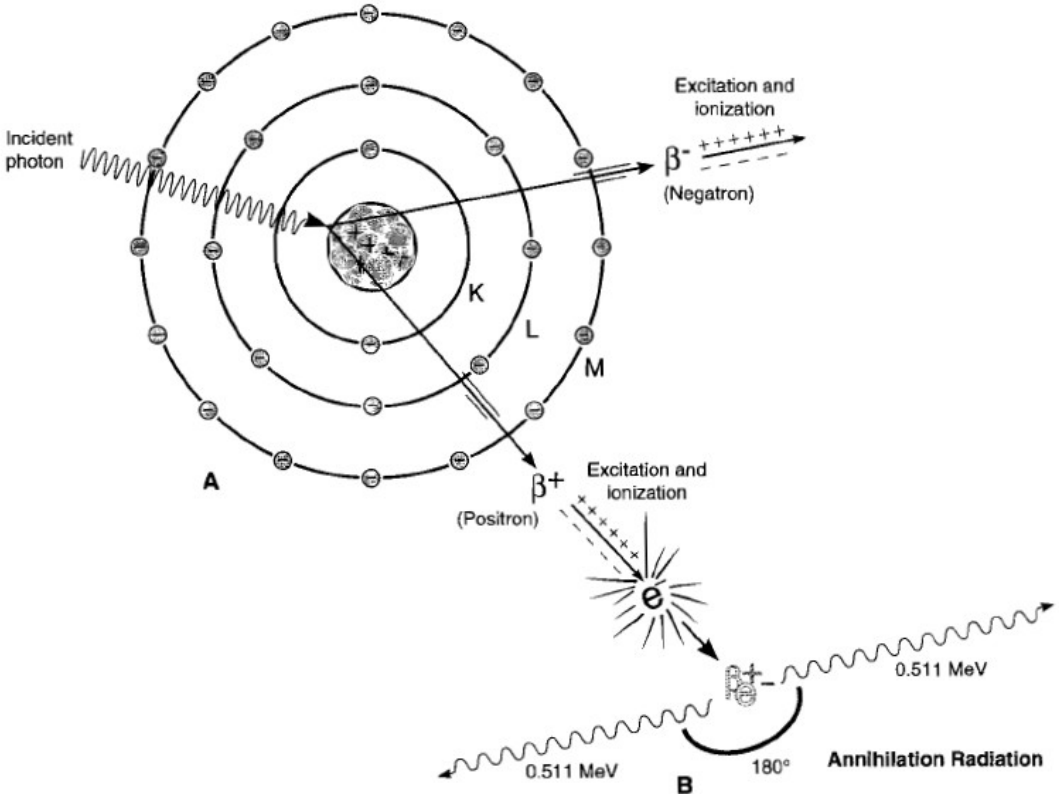

The diagram 2.8 illustrates the pair production process (Bushberg JT et al , 2002).

2.6.5 Photodisintegration (PD):

is the process by which the x-ray photon is captured by the nucleus of the atom with the ejection of a particle from the nucleus when all the energy of the x-ray is given to the nucleus. Because of the enormously high energies involved, this process may be neglected for the energies of x-rays used in radiography.

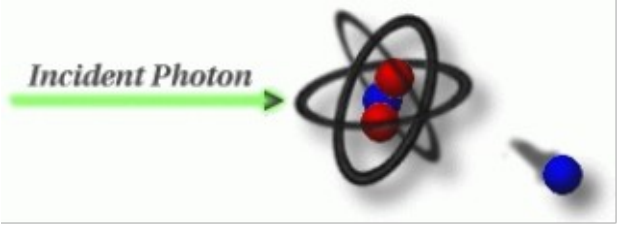

The figure (2-9) shows the Photodisintegration. (Murat Beyzadeoglu et al , 2010).

2.7 **Specific Features of X-Rays:**

X-rays are a type of electromagnetic radiation with wavelengths of 10–0.01 nm, frequencies of 30–30,000 pHz (1015 Hz), and typical photon energies of 100 eV–100 keV (Table 2.1).

Table 2.1 Features of X-rays of various energies. (Murat Beyzadeoglu et al , 2010).

Photon energy		Frequency (Hz)	Wavelength (pm, = 10^{-12} m)	Half-value layer (HVL)			
(keV)	(J)			Cement	Lead	Human body	Aluminum
1	1.602×10^{-16}	2.418×10^{17}	1,240	0.87 μm	0.117 μm	1.76 μm	2.17 μm
10	1.602×10^{-15}	2.418×10^{18}	124	147 μm	4.68 μm	1,220 μm	97.9 μm
100	1.602×10^{-14}	2.418×10^{19}	12.4	17.3 mm	0.110 mm	38.6 mm	15.1 mm
1000	1.602×10^{-13}	2.418×10^{20}	1.24	46.4 mm	8.60 mm	93.3 mm	41.8 mm
10,000	1.602×10^{-12}	2.418×10^{21}	0.124	132 mm	12.3 mm	298 mm	111 mm

X-rays are generally produced in either X-ray tubes or linacs. X-ray tubes are the main source of X-rays in laboratory instruments. In such a tube, a focused electron beam is accelerated under high voltage within a glass vacuum tube impacts a fixed or rotating target.

When the electrons approach target atoms, Coulomb interactions with the

nuclei cause the electrons to be suddenly deflected from their previous paths and slowed. During this braking process, energy in the form of X-rays is produced in a

continuous spectrum (bremsstrahlung X-rays). High-energy electrons hit inner orbital electrons and knock them out of the atom during the ionization process. Free electrons from outer orbits then fill the empty spaces in the inner orbitals, and X-rays with energies that are characteristic of the target are produced (**characteristic** X-rays) (Murat Beyzadeoglu et al , 2010).

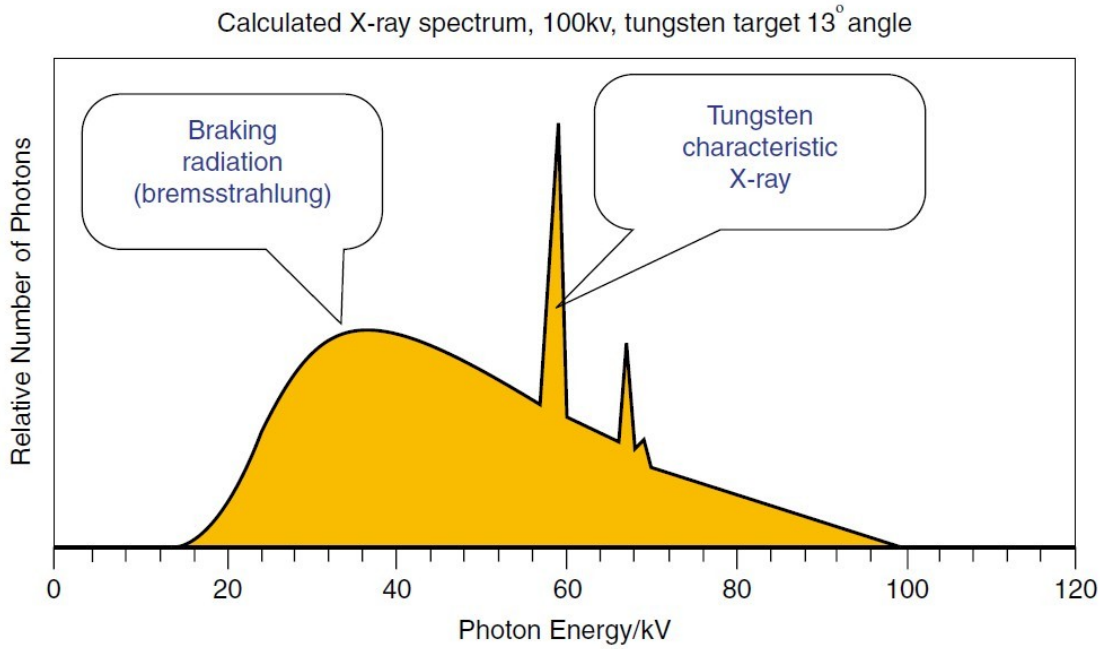

Fig. 2.10 X-ray spectrum (Murat Beyzadeoglu et al , 2010).

2.8.Anode Heel Effect:

Due to the absorption of x-rays by the anode heel the radiation intensity on the cathode side of the x-ray tube is higher than the anode side.

This effect is increased when the target angle is reduced It is generally accepted that an x-ray beam's intensity is not uniform throughout its entirety. As x- radiation is emitted from the target area in a conical shape, measurements have determined that the intensity in the direction of the anode (AC) is lower (over and above the difference caused by the Inverse Square Law) than the intensity in the direction of the cathode (AB). The fact that the intensities vary in such a manner causes visible differences in the

density produced on the radiographs. This phenomenon is called heel effect. (NRPB EXAM, 2000).

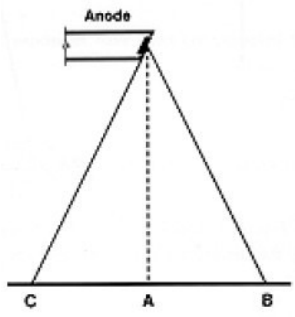

NOTE:
A = 100-percent intensity
AB = consists of a slight increase over 100-percent intensity and then a general decrease in intensity as B is approached
AC = consists of a considerable decrease in intensity as C is approached

The figure (2-11) shows the illustration of heel effect.

The decreased intensity at C results from emission which is nearly parallel to the angled target where there is increasing absorption of the x-ray photons by the target itself. This phenomenon is readily apparent in rotating anode tubes because they utilize steeply angled anodes of generally 17 degrees or less. Generally, the steeper the anode, the more severe or noticeable the heel effect becomes.

The effects of focus film distance on the visualization of heel effect are illustrated below:

Figure G

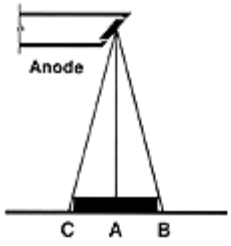

Figure H

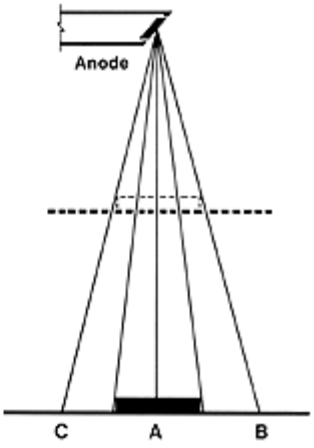

Figure (2-12) shows the film plane position.

Figure G shows the film plane as having a shorter focus film distance than the film plane in Figure H. Looking at Figure G, you can readily see that the x-ray beam's involvement in exposing the film runs from C to B (the full cone of radiation). Heel effect causes a greater decrease in x-ray beam intensity as one travels from the central ray to the cathode (A to B).

As you look at Figure H, note that a long focus film distance is used which results in the involvement of the x-ray beam at the film plane which does not utilize the full cone of radiation (C to B). Hence, the extremities of the beam (C and B) are not used in exposing the film. Because of this, heel effect is greatly reduced.

2.9. Applications

1. Intensity of beam on anode side is less than cathode side -therefore place the thicker part of body on cathode side, e.g. upper thoracic on anode side and lower thoracic or upper abdomen should be placed on cathode side.
2. Target-to-film distance - increase in distance reduces heel effect.
3. Size of film (keeping target-to-film distance as constant) - smaller film has lesser heel effect as the divergent beam does not reach the film and intensity of beam is more uniform at centre than at the periphery.

2.10. Influence of Anode heel effect:

The difference in the intensity can vary by as much as 45%.If the center is 100% the anode side of the beam can as low as 75% and the cathode as much as 120%.The heel effect should be considered when positioning areas of the body with different thickness or density. The cathode side should be over the area of greatest density. (R. Paydar et al, 2012).

2.11. Previous Studies:

J. F. D. S. Soares et al 2013 estimated the Attenuation of anode heel effect with an aluminum filter and their influence on patient dose in lumbar spine radiography, the study was done in the radiology service of Faro's health center, one of the many institutions in the Regional Health Administration of Algarve, Portugal. The study was applied in the conventional radiography of the lumbar spine, on a lateral position, since it's one of the examinations where, apparently, there's still a discrepancy in the image homogeneity, even if the patient is positioned so that this effect contributes for radiologic image quality. First, the parameters to be used in the lateral radiography of the lumbar spine were determined (voltage, current-time product, FFD, focus, etc.). These parameters were reproduced in order to study the anodic effect along the anode-cathode axis, on an exposition area of 40x20 cm and a table-focus distance of 90, 2 cm. The study began by performing some quality control tests, which were analyzed: the influence of the scattered radiation according to the variation of the exposition field size, the accuracy of the voltage and the real table-focus distance. The beam intensity along the longitudinal axis was also measured, for the characterization of the anodic effect. Analyzing the result varying flow of unfiltered dose, it appears that in the anode cathode region (positive axis) there's a decrease in the dose rate up to 58%. Not disregarding the influence of the scattered radiation in the test results, the slight decrease in intensity of the radiation on the edge of the cathode dues to the fact that the intensity is lower on the edges, meaning that the field area around the detector decreases as this approaches the edges.

With the filter applied to the output of the ampoule, it is noted that there is greater uniformity in the beam along the whole axis, with only a 9% variation between the

maximum and minimum value. The reduction in radiation intensity due to the decrease of the scattered radiation is also visible.

The addition of the filter also allowed attenuate the X-Ray beam, eliminating the low energy and contributing to a reduction in dose rate. For testing the filter effect on the image quality, conventional radiographies of the lumbar spine on a lateral position were performed, with the volunteer's head to the anode side, with and without filter.

A. Mehranian et al 2009 Quantitative assessment of the Effect of Anode Surface Roughness on Diagnostic X-ray Spectra: A Monte Carlo Simulation Study, An experimental measurement study involving surface profilometry and scanning electron microscopy (SEM) combined with MCNP4C-based Monte Carlo simulations was performed to evaluate anode surface roughness in aged x-ray tubes and to quantitatively predict its impact and relevance on generated diagnostic x-ray spectra. Surface profilometry determined that the center-line average roughness in the most aged x-ray tube evaluated in our study was around 50 μm. SEM measurements also revealed valuable details about the morphology of cracks and irregularities on the anode's focal path. An image-based modeling method was followed for defining more realistic models from the surface-cracked anodes into MCNP's environment. In this approach, the matrices of focal spot images were numerically processed such that the mean depth of cracks along with their spatial pattern to be incorporated into pixel values in agreement with the measured average depths. By invoking MCNP4C's Gaussian energy broadening (GEB), the correctness of this code in simulating diagnostic x-ray spectra was well validated against experimentally-measured spectra. The simulated spectra in surface deteriorated anode models were compared with those simulated in perfectly plain

anodes considered as reference. From these comparisons, an intensity loss of 4.5% and 16.8% was predicted for anodes aged by 5 and 50 μm-deep cracks in

conditions of 50 kVp, 6 degree target angle, 2.5 mm Al total filtration. By deploying several point detectors (F5 tallies) along the anode-cathode direction and averaging exposure over them, it was found that for a 12 degree anode roughened by 50 μm-deep cracks, the reduction of overall exposure is 14.9% and 13.1% for

70 and 120 kVp tube voltages, respectively. Finally, change in patient entrance skin dose (ESD), as a result of anode roughness, was assessed under various conditions in a chest x-ray radiography examination. In conclusion, anode surface roughness can have a non negligible effect on output spectra in aged x-ray imaging tubes and as such, depending on x-ray tube's workload, its impact should be carefully considered in medical x-ray imaging systems.

G. Behiels et al, 2001, Retrospective correction of the heel effect in hand radiographs, A method for retrospective correction of intensity inhomogeneities

Induced by the heel effect in digital radiographs is presented. The method is based on a theoretical model for the heel effect which is derived from the acquisition geometry. Because the heel effect is directly measurable in the direct exposure area only, the image is partitioned first to exclude collimation and diagnostic areas. The parameters of the model are determined by fitting the model to the direct exposure area and the correction is then applied to the whole image. The method iterates

between background segmentation and heel effect correction until convergence. We evaluate the suitability of the method on flat field and phantom images and demonstrate its robustness on a database of 137 diagnostic hand radiographs.

The method was tested on 137 digital hand radiographs, recorded with Agfa

ADC cassettes and Agfa ADC-MD10 & ADC-MD30 imaging plates and irradiated

by X-ray tubes Philips SRM 06 12 - ROT 500 or Siemens Bi 125/40 RL.

Results of the image partitioning procedure are. Visual inspection showed that the algorithm was able to correctly extract direct exposure, collimation and diagnostic areas for all images in our database. The time required to perform the partitioning was about 1 to 2 seconds using a Pentium III 800MHz on images resized to about 512 × 512 pixels.

Marcelo Zanchetta, et al, 2007, An Automatic Correction Method for the Heel effect in Digitized Mammography Images, A CGR 500T Stenograph radiological unit was used to produce all the test images. The system was equipped with a x-ray tube with a molybdenum anode (Mo), filter Mo, and a beryllium window producing a 0.3-mm nominal sized focus. Although the equipment contains an automatic exposure control system, the parameters were manually adjusted. Five aluminum disks, each with diameter of 10 mm and a thickness of 1.5 mm, were used as phantoms to produce 40 images. Kodak Min-R 2000 and Fuji AD-M films were used to provide high contrast and quality mammograms. The 180 × 240 mm films were reduced to 140 × 180 mm maintaining only the regions of interest and were subsequently digitized with a spatial resolution of 169 μ into 8 bits intensity levels with aVIDAR–Diagnostic Pro equipment providing adequate experimental data. To evaluate the proposed method, various data acquisition conditions were changed. The presented results show that the developed algorithm can efficiently determine the anode–cathode axis in all cases. The localization of the anode–cathode axis was evaluated with a correlation function. This correlation function permits the generation of a metric to compare the similarity between the simulated and the mammographic images. An average similarity of about 90% was obtained. This value is considered satisfactory by Dekker et al. in his evaluation of radiotherapy images.

The largest error with the proposed method used to define the position of the radiation center of the field parallel to the anode–cathode axis, even when it was compared to the measured position obtained with the commercial equipment, was

3.38 mm of the 180-mm analyzed region of interest. In the perpendicular direction, the largest observed error was 3.89 mm of the 140-mm region of interest. However, the method differs on average by 2.49 mm (1.78% of the image) in the direction perpendicular to the anode–cathode axis and 2.02 mm (1.12% of the image) parallel to the axis.

The small differences between the obtained results of the two methods can be attributed to: quantum noise, digitalization, and processing inaccuracies. The influence of these errors on the performance of the method was also analyzed. Three-dimensional representations of the pixel density distributions of the corrected images indicates that the method is capable of obtaining uniform background regions, maintaining the contrast of the objects, obtaining better results than those presented by majority of the traditional techniques for the correction of nonuniform illumination.

A quantitative study of the density variations of the background of the images shows that our method was also efficient in removing background noise; capable of reducing the noise to an average of 94.55%.

Chapter Three

Materials and Methods

3.1Materials:

3.1.1. Phantom:

in this study, dry femur and humerus phantom was used to obtain image.

3.1.2. Densitometer:

In this study, the densities of image obtained by measuring using densitometer.

3.1.3. X-ray Unit:

In this study, three different modalities X-ray machines, from different manufacture were used as described in Table 3.1

Table 3.1. Show X-rays equipments specifications.

Center	Manufacturer	Manufactu-ring Date	Type	Focal spot (mm)	Max KVp	Max mA	Max time (s)
MMC	Fujifilm	Jan 2013	fixed	1.5/.6	150	250	.8
ANTALIA	Toshiba	Aug 2003	Fixed	0.6-1.2	150	500	2.5
ENT	Shimadzu	April2007	Fixed	1-2	150	500	2

3.2. Methods

3.2.1. Study duration:

This study performed in period of June to December 2014

3.2.2. Study place:

This study conducted in Modern Medical Center Hospital , Antalia Center Hospital and Ear Nose and thorat hospital.

3.2.3. Method of data collection:

In this study femur and humerus dry phantom are exposed, , the image was obtained using dry phantom in the Modern Medical Center, Antalia Center , Ear Nose and thyroid hospital with marks in Anode side and cathode side. the quantitative measurement of optical density in light-sensitive materials(film) The radiographic equipment used was Shimadzo imaging system. Total filtration for the X-ray system was measure as 2.7 mm of aluminum equivalent. A single exposure control system was available for use in the standing position.

3.2.4. Image Evaluation:

Densitometer and Visual inspection are used to evaluate the heel effect of x-ray machine, by measuring the image densities. The evaluation of the images was done by survey questionnaire involve the asking (50) professional radiologist to identify the optical density and their opinion about the image densities

3.2.5. Method of data analysis:

The data was analyze with excel program.

Chapter Four: The Results

In the following table and graphs data of study are presented the optical

density of images.

The table (4-1) shows the mean values of optical density for the femur images at thicker part to the Anode.

Image Technique	Position of the measured intensity		
	Anode Side (Mean ± Standard deviation)	Cathode Side (Mean ± Standard deviation)	Middle Side (Mean ± Standard deviation)
Manual Processing	1.23±.01414	1.28±0.04243	1.44±00.00
Digital Radiography (DR)	1.22± 0.13077	1.05± 0.03	1.33± 0.01
Computer Radiography (CR)	1.76±0.04243	1.925±0.10607	2.07±0.02828

Figure (4.1) shows the correlation between the cathode optical density and anode optical density for the femur images at thicker part to the anode.

The figure (4-2) show the mean values of optical density for the femur images at thicker part to the anode for different imaging techniques.

The table (4-2) shows the mean values of optical density for the femur images at thicker part to the cathode.

Image Technique	Position of the measured intensity		
	Anode Side (Mean ± Standard deviation)	Cathode Side (Mean ± Standard deviation)	Middle Side (Mean ± Standard deviation)
Manual Processing	1.835± 0.02121	1.905± 0.00707	2.02± 0.01414
Digital Radiography (DR)	1.265± 0.07778	1.065± 0.13435	1.26 ± 00.00
Computer Radiography (CR)	2.335± 0.02121	2.39± 00.00	2.355± 0.00707

Figure (4.3) shows the correlation between the cathode optical density and anode optical density for the femur images at thicker part to the cathode.

The figure (4-4) show the mean values of optical density for the femur images at thicker part to the cathode for different imaging techniques.

Image Technique	Position of the measured intensity		
	Anode Side (Mean ± Standard deviation)	Cathode Side (Mean ± Standard deviation)	Middle Side (Mean ± Standard deviation)
Manual Processing	1.005± 0.07778	1.25± 0.01414	1.34± 0.01414
Digital Radiography (DR)	1.50667±0.08386	1.61± 0.32909	1.46 ± 0.09899

Figure (4.5) shows the correlation between the cathode optical density and anode optical density for the humorous images at thicker part to the anode.

The figure (4-6) shows the mean values of optical density for the humerus images at thicker part to the anode for different imaging techniques.

The table (4-4) shows the mean values of optical density for the humerus images at thicker part to the cathode.

Image Technique	Position of the measured intensity		
	Anode Side (Mean ± Standard deviation)	Cathode Side (Mean ± Standard deviation)	Middle Side (Mean ± Standard deviation)
Manual Processing	1.065± 0.0495	1.255± 0.00707	1.305 ± 0.02121
Digital Radiography (DR)	1.805± 0.02121	1.72 ± 0.01414	1.78 ± 00.00

Figure (4.7) shows the correlation between the cathode optical density and anode optical density for the humorous images at thicker part to the cathode.

The figure (4-8) show the mean values of optical density for the humerus images at thicker part to the cathode for different imaging techniques.

The table (4-5) shows the mean values of optical density for the exposed film.

Image Technique	Position of the measured intensity		
	Anode Side (Mean ± Standard deviation)	Cathode Side (Mean ± Standard deviation)	Middle Side (Mean ± Standard deviation)
Manual Processing	0.87± 0.01414	0.97± 0.00707	0.94 ± 0.01414
Digital Radiography (DR)	0.32± 0.01414	0.40 ± 0.01414	0.36 ± 0.01414

Figure (4-9) shows the mean values of optical density for the exposed film for DR and CR.

The table (4-6) shows the visual inspection .

Image Intensity	***Frequency***	***Percentage %***
more Intensity Anode	05	10%
Cathode more Intensity	12	24%
Same Intensity	33	66%

Figure (4-10) shows the visual inspection.

Chapter Five

Discussion, Conclusion and Recommendation

5.1 Discussions:

This study used to evaluate the effect of Anode heel in conventional X-ray tube in image quality, and densities along the axis of x-ray tube. The main results were that the densities increase toward cathode except in digital radiography, which are the same identify in literature, also the variation in densities is due to the variation in x-rays intensities but this will not affect on image quality especially in DR, due to wide capability of post processing of the image which result in enhancing image contrast and visibility and reduced the effect of x-ray intensities variation. A total of 10 images was obtained using dry phantom, the exposure factors used to obtain the image, 50 (Kvp), 5 current time product (mAs), and the ESDs was established at a reference point of 100 cm from tube focus for the range of current time product (mAs) and tube potentials encountered in clinical practice. Optical density is a result of the darkness of a developed picture and can be expressed absolutely as the number of dark spots in a given area, but usually it is a relative value, expressed in a scale.

5.2 Conclusion:

The density increase toward cathode side, which approved in two techniques used film screen, computed radiography, but in digital radiography this phenomena is not correct, due to the wide capability of post processing to enhance contrast and densities.

5.3 Recommendation:

- In diagnostic radiography heel effect must be considered that the intensity of the beam is stronger toward the cathode, so if the patient is unequal in thickness, the denser or thicker portion of the body should be positioned toward the cathode.
- In diagnostic radiography heel effect must be considered that the heel effect will be much less noticeable if the focal-film distance is large. Conversely, if the focal-film distance is shortened, the effect of the unequal intensity within the x-ray beam will be noticed greatly.

- In diagnostic radiography heel effect must be considered that the heel effect will be noticed when exposing a large film while not as obvious when exposing a small film.
- Practical guidelines for better image quality in computed radiography and digital radiography is mainly concerned with the professional skills of the users and the establishment of an efficient quality control program specifically designed to produce the best quality of clinical images.

5.4 References:

Bushberg, J.T.; Seibert, J.A.; Leidholdt, E..M, & Boone, J.M. The Essentials Physics ofMedical Imaging. New York: Lippincott Williams & Wilkins, 1997:.

Bushong, S.C. 2002: *Radiologic Science for Technologists* S1. Louis: Moshy.

Curry TS, Dowdey JE, Murry RE. Christensen´s physics of diagnostic radiology 4 Ed. Lippincott Williams & Wilkins. (1990) ISBN:0812113101.

E.B. Podgorsak ,Radiation Oncology Physics: A Handbook for Teachers and Students ,Technical Editor 2005.

E.B. Podgorsak Radiation physics for medical physicist 2006.

European Commission: European Commission. European Guidelines on Quality Criteria for Diagnostic Radiographic Images. 1996, EUR 16260 EN.

Garmer M, Hennings SP, Jäger HJ, et al. Digital radiography versus conventional radiography in chest imaging: diagnostic performance of a large-area flat-panel detector in a clinical CT-controlled study. AJR 2000; 174: 75-80

Murat Beyzadeoglu • Gokhan Ozyigit • Cuneyt Ebruli, Basic Radiation Oncology 2010

National Radiological Protection Boared: *Doses to Patients from Medical X-ray Examinations in the UK*. 2000, NRPB.

Pam Cherry and Angela Duxbury Practical radiotherapy physics and Equipment , Second Edition
,2009.

Radiation Risks and Realities: EPA-402-K-07-006, Environmental Protection Agency Office of Radiation and Indoor Air May 2006

R. Paydar1,3, A. Takavar1, M.R. Kardan2,3, A. Babakhani3,4, M.R. Deevband3, S. Saber5, Patient effective dose evaluation for chest X-ray examination in three digital radiography centers, *Iran. J. Radiat. Res., 2012; 10(3-4): 139-143.*